Quantum Zeno effect induced by quantum-nondemolition measurement of photon number

M.J.Gagen and G.J.Milburn
Department of Physics, University of Queensland, St. Lucia 4072, Australia
(Received 4 November 1991)

Measurements performed on a system will alter the dynamics of that system, and in the strong-measurement limit, can theoretically freeze the free evolution completely. This is the quantum Zeno effect. We utilize quantum-nondemolition photon-counting techniques to realize the Zeno effect on the evolution of either a two-level Jaynes-Cummings atom interacting with a resonant cavity mode, or on two electromagnetic modes configured as a multilevel parametric frequency converter. These systems interact with another electromagnetic cavity mode via a quadratic coupling system based on four-wave mixing and constructed so as to be a nondemolition measurement of the photon number. This mode is then coupled to the environment through the cavity mirrors. This measurement is shown to be a measurement of system populations, which generates the desired Zeno effect and in the strong-measurement limit will freeze the free dynamics of the system.

PACS number(s): 42.50.Md, 03.65.Bz

I. INTRODUCTION

Unlike classical mechanics, measurements are given a special status in quantum mechanics; it cannot be assumed that the effect of measurement on the system can be made arbitrarily small. This is a direct result of the noncommutativity of the operators that represent the physical variables in quantum mechanics. From the very earliest days of quantum mechanics it was necessary to supplement quantum theory with additional postulates, generally referred to as projection postulates, which describe the effect of measurement. The essential feature of these postulates is their nonunitary character. The projection postulates describe a very general, highly idealized class of measurements, corresponding to instantaneous, arbitrarily accurate readouts. The probability distributions for such measurements are given directly by projecting the quantum state of the system onto the appropriate eigenstates of the operator corresponding to the measured quantity, without any reference to the details of the measurement scheme. This degree of generality suggests that such measurements should be seen more as part of the interpretation of quantum theory than as a realistic description of the measurement process.

It has been known for some time that such idealized measurements can dramatically alter the free dynamics of systems with a discrete spectrum [1, 2]. In particular a two-level system undergoing coherent oscillations between the two states, subjected to a sequence of projective measurements, can be frozen in the initial state [3], the so-called quantum Zeno effect. This extreme result is a direct consequence of the extreme idealization such projective measurements embody; real measurements are neither instantaneous nor arbitrarily accurate. Recently the theory of measurement has been supplemented by mathematical results which enable these restrictive assumptions to be discarded[4–6]. In particular it is now possible to describe a more general class of measurements which are not arbitrarily accurate. In Ref. [3] one of us showed that the effect of a sequence of inaccurate, instantaneous measurements on the two-level system could be described by a Markov master equation for the system state. In an appropriate limit, defining an efficient measurement, the initial-state occupation probability decays exponentially linearly in time with a very slow rate. This is a manifestation of the quantum Zeno effect in a more realistic way.

There has only been one attempt to verify the quantum Zeno effect [7]. The main difficulty to be overcome in searching for an experimental realization of the quantum Zeno effect is arranging for the measurement time scales to be much shorter than the time scales of any other nonunitary effect such as dissipation. Recently we proposed a scheme based on Rydberg atoms in a microwave cavity which may provide just this situation [8]. In this paper we discuss two other quantum-optical models, a parametric frequency conversion model and a Jaynes-Cummings model, which offer some hope of experimental realization. In addition the parametric frequency conversion model requires more than two levels to describe the free dynamics. We thus are provided with the opportunity of studying how the quantum Zeno effect is manifest in multilevel systems. Aspects of the Zeno effect in multilevel systems were recently discussed by Peres [9].

In the Jaynes-Cummings model we assume that the atom is initially prepared in the excited state and the field in the vacuum state. The coupling between the atom and the field is such that the atom periodically emits one photon into and absorbs one photon from the cavity mode. The objective is to monitor the initial state of the atom by watching for this photon to appear in the cavity mode. If the Zeno effect occurs the probability of finding the photon in the cavity mode should become a very slowly increasing function of time. In the para-

metric frequency conversion model we prepare one mode in a vacuum state and the other mode in an N_p photon number eigenstate. As the evolution proceeds these N_p photons are exchanged between each of the two interacting modes. We monitor the initial state by measuring the photon number in the initially unexcited cavity mode.

In studying the effect of measurement on free dynamics it is useful to reduce the effect of measurement to the least possible disturbance permitted by quantum mechanics. In this respect quantum nondemolition measurements seem particularly interesting. It is the purpose of an ideal quantum nondemolition measurement to yield a determinate sequence of measured results [10]. For this to be possible it is essential that an initial accurate measurement of some physical quantity does not feed noise into the system in such a way that it is coupled back into the measured variable. Such a situation would produce a subsequent measurement result which could not be related in a deterministic way to the initial result. Variables which avoid this noise feedback are referred to as quantum-nondemolition (QND) variables. Constants of motion are of course QND variables, provided such variables remain constants of the motion in the presence of the interaction with the measuring device. This latter criterion is referred to as back-action evasion. In this paper we will consider QND measurements of photon number of an intracavity mode. Such measurements do not lead to any systematic damping in the system but do drive diffusion processes in dynamical variables which do not commute with the photon number, such as phase. We will use a QND measurement of the photon number in an optical cavity to monitor the evolution of a system away from the initial state.

II. FREE DYNAMICS

We consider two quantum-optical models, one based on the nondegenerate parametric frequency convertor [11, 12], the other on the Jaynes-Cummings model [13]. The first of these models describes the interaction of two intracavity field modes via a second-order nonlinear susceptibilty. The second describes the interaction between a single cavity mode and a two-level atom, in the rotating-wave and dipole approximation. As we shall show it is possible to describe the free dynamics of both these systems in terms of the precession of an abstract angular momentum vector, and we thus refer to both systems collectively as the rotation system.

We consider first a Jaynes-Cummings two-level atom interacting with a cavity of the radiation field described by [13]

$$\hat{H}_{\rm JC} = \frac{\hbar\kappa}{2}(b\sigma^{+} + b^{\dagger}\sigma^{-}), \tag{2.1}$$

where b ($b^{\dagger}$) are the annihilation (creation) operators of the b-mode cavity field, and κ is the dipole coupling strength of the atom-field interaction. The σ's are the usual operators of the su(2) Lie algebra defined by

$$\begin{aligned}\sigma_x &= \tfrac{1}{2}(|1\rangle\langle 2| + |2\rangle\langle 1|),\\ \sigma_y &= \frac{-i}{2}(|1\rangle\langle 2| - |2\rangle\langle 1|),\\ \sigma_z &= \tfrac{1}{2}(|2\rangle\langle 2| - |1\rangle\langle 1|).\end{aligned} \tag{2.2}$$

For the second rotation system we consider the coupling of two electromagnetic field modes in a nonlinear crystal. To obtain this interaction we might configure a second-order susceptibility as a parametric frequency converter [11, 12]. We have

$$\hat{H}_{\rm FC} = \frac{\hbar\kappa}{2}(a^{\dagger}b + ab^{\dagger}). \tag{2.3}$$

Here b is the same cavity mode given above, but the two-level atom is replaced by a further cavity mode with annihilation operator a. The coupling constant κ is proportional to the second-order susceptibility.

A simple way to describe the dynamics of the two-mode parametric frequency converter is to introduce the Hermitian operators [14, 15]

$$\begin{aligned}\hat{J}_x &= \tfrac{1}{2}(a^{\dagger}b + ab^{\dagger}),\\ \hat{J}_y &= \frac{-i}{2}(a^{\dagger}b - ab^{\dagger}),\\ \hat{J}_z &= \tfrac{1}{2}(a^{\dagger}a - b^{\dagger}b).\end{aligned} \tag{2.4}$$

These operators satisfy the usual su(2) Lie algebra of $[\hat{J}_x, \hat{J}_y] = i\hat{J}_z$, together with the cyclic permutations of x, y, and z. The Casimir invariant for this group is

$$\hat{J}^2 = \frac{\hat{N}_p}{2}\left(\frac{\hat{N}_p}{2} + 1\right), \tag{2.5}$$

where $\hat{N}_p$ is the total number of photons in the a and b modes,

$$\hat{N}_p = a^{\dagger}a + b^{\dagger}b. \tag{2.6}$$

It is also of interest to note that the photon number operator for the b mode can be written in terms of these angular momentum operators. We have

$$\hat{n}_b = \tfrac{1}{2}(\hat{N}_p - 2\hat{J}_z). \tag{2.7}$$

Using the above notation we can write the Hamiltonian of the rotational systems as

$$\hat{H}_{\rm rot} = \begin{cases}\hat{H}_{\rm JC} = \dfrac{\hbar\kappa}{2}(b\sigma^{+} + b^{\dagger}\sigma^{-})\\ \hat{H}_{\rm FC} = \hbar\kappa\hat{J}_x,\end{cases} \tag{2.8}$$

where we write JC to refer to the Jaynes-Cummings two-level atom model, and FC to refer to the frequency converter model.

We can readily show for the frequency converter model that the operator $\hat{N}_p$ (the total photon number occupancy of both modes) is a constant of motion as it commutes with the above Hamiltonian. For the Jaynes-Cummings model the equivalent conserved quantity is given in terms of the operator $\sigma_z + \hat{n}_b$.

For the Jaynes-Cummings two-level atom with one photon ($N_p = 1$), the basis states are given by the usual

$j = \frac{1}{2}$ spin eigenstates of the σ_z operator. With the above Hamiltonian the b mode can have at most zero or one photon in it, and therefore the atom–b-mode system is spanned by two basis vectors,

$$|\mathrm{I}\rangle \equiv |\tfrac{1}{2}\rangle_{\mathrm{atom}} \otimes |0\rangle_b, \qquad |\mathrm{II}\rangle \equiv |-\tfrac{1}{2}\rangle_{\mathrm{atom}} \otimes |1\rangle_b. \tag{2.9}$$

The number of available states is $N_s = N_p + 1$. We choose to prepare the system in the initial state $|I\rangle$ with the atom initially excited ($j = \frac{1}{2}$) and the b mode initially in the vacuum state. We note here that the combined Jaynes-Cummings atom and b-mode system is effectively a two-level system and will share many features with the frequency converter system for the case $N_p = 1$ and $N_s = 2$.

In Fig. 1 we plot the probability to find the system in the initial state versus the scaled time for two values of N_s. Clearly evident in Fig. 1(a) is the periodic oscillation between the initial state and the state in which the atom is deexcited and the field has one photon. We can thus monitor the evolution away from the initial state by monitoring the photon number inside the cavity.

For the two-mode frequency converter system we choose as basis states the eigenstates of $\hat{J}_z$. These are $|j, j-m\rangle$ where $j = N_p/2$ and $m = 0, 1, 2, \ldots, 2j$. In terms of the number states of modes a and b this is

$$|j, j-m\rangle \equiv |2j-m\rangle_a \otimes |m\rangle_b. \tag{2.10}$$

We prepare the frequency converter system with the b mode in the vacuum and the a mode in a number state with N_p photons:

$$|\Psi^{IN}\rangle_{a,b} \equiv |j, j\rangle \equiv |N_p\rangle_a \otimes |0\rangle_b. \tag{2.11}$$

The free dynamics of this system is described by a precession of the angular momentum about the J_x axis. When $\kappa t = \pi$ the state of the system is in the down angular momentum state $|j, -j\rangle$. In terms of the photon number representation this corresponds to the state in which mode a is in the vacuum state and mode b has exactly N_p photons, i.e., $|0\rangle_a \otimes |N_p\rangle_b$. In Fig. 1(b) we plot the probability to find the system in the initial state versus the scaled time for values of $N_p = 39$ or $N_s = 40$. Clearly evident is the perfect recurrence of the initial state as the precession of the angular momentum vector makes one complete revolution. Note that the rate at which the system leaves the initial state is much faster when N_p is large than is the case for only two levels ($N_p = 1$). As we shall show this has important implications for the appearance of the Zeno effect in such systems. To monitor the evolution away from the initial state once again we monitor the photon number in the b mode.

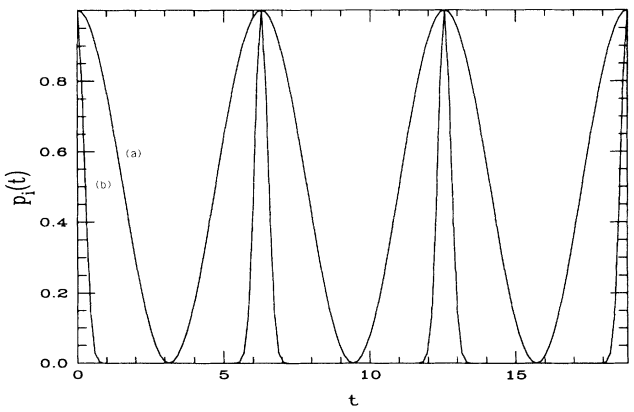

FIG. 1. The free-evolution initial-state occupancy probability for the case of $N_s = 2$, line (a), and the case $N_s = 40$, line (b). The two-level case applies equally well to the Jaynes-Cummings atomic system and the one-photon frequency converter system. Line (b) applies to the $N_p = 39$ photon frequency converter system. Here we set $\kappa = 1$. For (a) $p_i(0) = \langle I|\rho|I\rangle$, for (b) $p_i(0) = \langle j, j|\rho|j, j\rangle$.

III. MEASUREMENT MODEL

In both models discussed above it is necessary to monitor the photon number in the b mode, which is initially prepared in the vacuum state. In this section we describe how this quantity may be measured without absorbing b mode photons (a QND number measurement). This should represent the least disturbing measurement we can make. To achieve this we couple the rotation system to a third field mode c via a quadratic coupling scheme based on four-wave mixing. This later field mode plays the role of the first stage of the measuring device and we thus refer to it as the "detector." In both cases the interaction with the detector is a back-action evasion coupling with respect to the photon number in the other b mode.

However this is still not a measurement model. The next step is to couple the detector to the many-mode field external to the cavity. This coupling leads directly to nonunitary evolution of the entire coupled system-detector system. Of course we do not have a choice as to the nature of the coupling to the external cavity field; it is mediated by the output mirrors of the optical cavity. The effect of this coupling on the system-detector dynamics may be described, at optical frequencies, by a Markov master equation. This equation describes amplitude damping of the detector mode. However we are primarily interested in the dynamics of the system alone. With this object in mind the next step in the calculation is to obtain an effective evolution equation for the reduced state of the system. It is at this stage that we see the appearance of terms which lead to the diagonalization of the system density operator in the photon number basis, that is, in the basis which diagonalizes the measured QND variable.

The total Hamiltonian in the interaction picture is

$$\hat{H}_{\mathrm{tot}} = \hat{H}_{\mathrm{rot}} + \hat{H}_{\mathrm{QND}} + \hat{H}_{\mathrm{damp}}, \tag{3.1}$$

where $\hat{H}_{\mathrm{rot}}$ describes the free dynamics of either system, $\hat{H}_{\mathrm{QND}}$ describes the back-action evasion to the detector mode, and $\hat{H}_{\mathrm{damp}}$ describes the coupling of the detector mode to the field external to the cavity.

We introduce a QND-type coupling between the b mode and a third cavity mode, with annihilation operator c. The coupling is via a third-order susceptibility. In the interaction picture we have

$$\hat{H}_{\mathrm{QND}} = \frac{\hbar\chi}{2} b^\dagger b(c + c^\dagger), \tag{3.2}$$

where we choose χ to be real. This could be realized as a four-wave-mixing interaction with one of the modes treated classically [16–18], in which case χ is proportional to the third-order nonlinear susceptibility.

The above Hamiltonians when combined give a complicated but still straightforward unitary evolution, and thus do not describe a measurement. We now need to couple the detector mode c to the many-mode field external to the cavity. Ordinary photon-counting measurements are made directly on the field which leaves the cavity. The detector mode and external field comprise the total measuring device. We shall return to this point in Sec. IV. The interaction between the detector field and the external field is described by the interaction Hamiltonian

$$\hat{H}_{\mathrm{damp}} = c\Gamma^\dagger + c^\dagger\Gamma, \tag{3.3}$$

where Γ are bath operators describing the many-mode external field. In Fig. 2 we give a diagrammatic representation of the system-detector-environment complex.

We are now in a position to write down the evolution equation for the state of the system and detector. To do this we use standard techniques [19] to eliminate the dynamics of the external field, yielding a master equation

$$\dot{\hat{\rho}} = \frac{-i}{\hbar}[\hat{H}_{rot}, \hat{\rho}] - i\chi[\hat{n}_b\hat{X}_c, \hat{\rho}] + \frac{\gamma}{2}(2c\hat{\rho}c^\dagger - \hat{n}_c\hat{\rho} - \hat{\rho}\hat{n}_c), \tag{3.4}$$

where $\hat{n}_c$ is the number operator for the c mode and $\hat{X}_c = \frac{1}{2}(c + c^\dagger)$ is the quadrature phase operator for the c mode. Here we have treated the dissipation resulting from the coupling of the c mode to the environment under the Markov approximation.

To describe the dominant effect of the coupling to the measuring device we first consider the case in which $\kappa = 0$, i.e., we turn off the free dynamics. The solution to the master equation in this case was obtained by Walls, Collet, and Milburn [16]. When $\kappa = 0$ then n_b is a constant of the motion as there is no mechanism to shift photons from the a to the b mode. They considered an initial state with the b mode prepared in an arbitrary state and the c mode prepared in a vacuum,

$$\hat{\rho}_{bc}(0) = \sum_{n,m} \rho_{n,m}|n\rangle_b\langle m| \otimes |0\rangle_c\langle 0|, \tag{3.5}$$

and obtained for the density matrix at time t,

$$\rho_{bc}(t) = \sum_{n,m} \rho_{n,m} \exp\left[\frac{\chi^2}{\gamma^2}(n-m)^2\left(1 - \frac{\gamma t}{2} - e^{-\gamma t/2}\right)\right] \times |n\rangle_b\langle m| \otimes \frac{|\alpha_n(t)\rangle_c\langle\alpha_m(t)|}{\langle\alpha_m(t)|\alpha_n(t)\rangle_c}, \tag{3.6}$$

where $|\alpha_n(t)\rangle_c$ denote coherent states of the c mode with

$$\alpha_n(t) = \frac{-i\chi n}{\gamma}(1 - e^{-\gamma t/2}). \tag{3.7}$$

Here we see that the c mode has been driven into a superposition of coherent states. In turn, the damping of the c mode has introduced the exponential factor dependent on $(n-m)^2$ which will damp the coherences of the b mode density matrix in the number basis. This result is typical of measurement schemes which destroy coherences and leave the system in a mixture of states in the measurement pointer basis, in this case the b mode number states. In the limit $\gamma t \gg 1$ the coherence decay is exponential with the decay rate given by $\chi^2(n-m)^2/2\gamma$. This would seem to indicate that a good measurement corresponds to having $\chi^2 t/\gamma$ very large where t is the measurement time. Indeed in the Appendix we show that in this limit the signal-to-noise ratio for the measurement

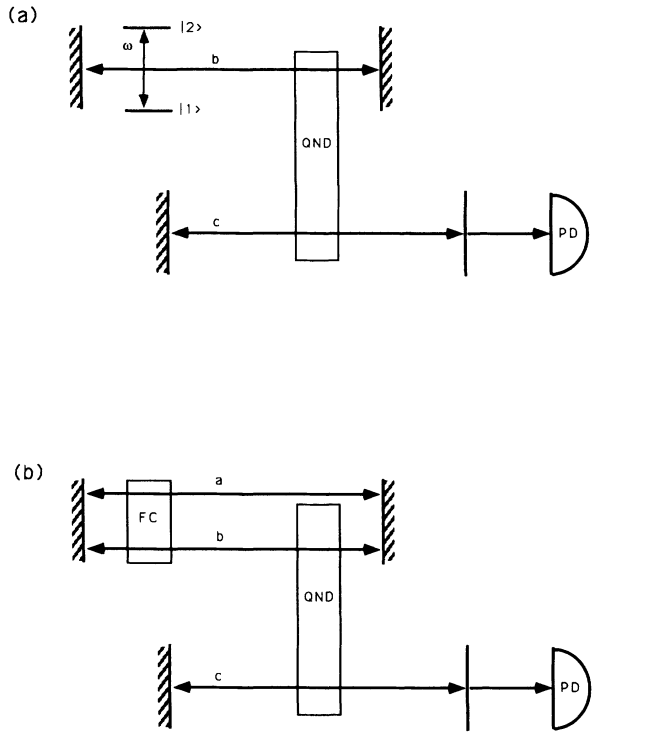

FIG. 2. The schematic experimental arrangement is shown for the Jaynes-Cummings two-level atom system (a), and for the two-mode frequency converter system (b). In (a) the two-level atom is tuned to the cavity mode b. In (b) the cavity supports two modes a and b interacting through a second-order susceptibility so as to be configured as a parametric frequency converter (shown as FC). In both systems then, mode b is coupled to another electromagnetic cavity mode, c via a quadratic coupling system based on four-wave mixing and constructed so as to be a nondemolition measurement of the quadrature phase (shown as QND). Photon number counting is then performed on this third mode c (shown as PD).

is very good. For $\gamma t \gg 1$ with large damping rate a good measurement means that $\chi^2 t \gg 2\gamma$. As well, for large γ we are motivated to consider the possibility of adiabatically eliminating the detector mode from the dynamics and obtaining an evolution equation for the system alone.

When $\kappa \neq 0$ the above analysis suggests the mechanism by which the Zeno effect is manifest. The damping of the c mode rapidly eliminates the off-diagonal coherences in the photon number distribution and it is precisely these coherences that need to "build up" in order for the unitary rotation of the free evolution part of the system to occur.

IV. ADIABATIC ELIMINATION OF THE DETECTOR MODE

In this section we treat the large-damping limit ($\gamma t \gg 1$). In this limit we make an ansatz for the state of the c mode, and by adiabatically eliminating this mode obtain a reduced master equation for the evolution of the remaining system—the two-level atom and b mode in the Jaynes-Cummings case, or the a and b modes in the frequency converter case.

We are interested in the large-damping regime on the c mode where we are rapidly and destructively counting all the photons that are generated in the c mode. We expect, based on this, that the c mode is never able to evolve very far away from the vacuum. This provides the basis of the adiabatic method we are going to consider. There are various schemes to do this and we choose to follow the method used by Mortimer and Risken [20].

For large γ the c mode is heavily damped and remains close to the vacuum state $|0\rangle_c\langle 0|$. A photon number expansion of Eq. (3.6) indicates that this is readily satisfied in the limit $\gamma \gg \chi$. In what follows we allow for small deviations from the vacuum in setting

$$\rho_{\rm tot} = \rho_0 \otimes |0\rangle_c\langle 0| + \rho_1 \otimes |1\rangle_c\langle 0| + \rho_1^\dagger \otimes |0\rangle_c\langle 1| + \rho_2 \otimes |1\rangle_c\langle 1|, \tag{4.1}$$

where ρ_0, ρ_1, $\rho_1^\dagger$, and ρ_2 are operators with respect to either the a and b modes in the frequency converter case, or to the b mode and σ operators in the two-level atom case. We also note that the reduced density operator for the a and b modes is

$$\rho_{\rm rot} = {\rm tr}_c(\rho_{\rm tot}) = \rho_0 + \rho_2. \tag{4.2}$$

When we insert Eq. (4.1) into the total system master equation (3.4) and collect terms in $|0\rangle_c\langle 0|$, $|1\rangle_c\langle 0|$ and $|0\rangle_c\langle 1|$ and $|1\rangle_c\langle 1|$ we obtain

$$\begin{aligned}
\dot\rho_0 &= \frac{-i}{\hbar}[H_{\rm rot}, \rho_0] - \frac{i\chi}{2}[\hat n_b \rho_1 - \rho_1^\dagger \hat n_b] + \gamma\rho_2, \\
\dot\rho_1 &= \frac{-i}{\hbar}[H_{\rm rot}, \rho_1] - \frac{i\chi}{2}[\hat n_b \rho_0 - \rho_2 \hat n_b] - \frac{\gamma}{2}\rho_1, \\
\dot\rho_1^\dagger &= \frac{-i}{\hbar}[H_{\rm rot}, \rho_1^\dagger] - \frac{i\chi}{2}[\hat n_b \rho_2 - \rho_0 \hat n_b] - \frac{\gamma}{2}\rho_1^\dagger, \\
\dot\rho_2 &= \frac{-i}{\hbar}[H_{\rm rot}, \rho_2] - \frac{i\chi}{2}[\hat n_b \rho_1^\dagger - \rho_1 \hat n_b] - \gamma\rho_2.
\end{aligned} \tag{4.3}$$

To obtain these equations we discarded all terms involving the matrix elements $|0\rangle_c\langle 2|$ and $|2\rangle_c\langle 0|$. Here we see the essence of the adiabatic approximation in that for large γ, ρ_1 and $\rho_1^\dagger$ are heavily damped.

Using Eq. (4.2) we have for the reduced density operator

$$\dot{\hat\rho}_{\rm rot} = \frac{-i}{\hbar}[H_{\rm rot}, \rho_{\rm rot}] - \frac{i\chi}{2}[\hat n_b, \rho_+], \tag{4.4}$$

where $\rho_+ = \rho_1 + \rho_1^\dagger$. The adiabatic approximation is made by setting $\dot{\hat\rho}_1 = \dot{\hat\rho}_1^\dagger = 0$. This approximation amounts to a slaving of the fast variables for large damping ($\gamma t \gg 1$) to the slow ones. If we substitute these results into Eqs. (4.3) we obtain

$$\hat A = F(\hat\rho_+) = \Big(\hat\rho_+ + i\mu[H_{rot}, \hat\rho_+]\Big), \tag{4.5}$$

where

$$\hat A = -\frac{i\chi}{\gamma}[\hat n_b, \hat\rho_{ab}] \tag{4.6}$$

and $\mu = 2(\hbar\gamma)^{-1}$. We invert this equation to obtain

$$\begin{aligned}
\hat\rho_+ &= F^{-1}(\hat A) \\
&= \hat A - i\mu[H_{\rm rot}, \hat A] - \mu^2[H_{\rm rot}, [H_{\rm rot}, \hat A]].
\end{aligned} \tag{4.7}$$

We expand $\hat\rho_+$ to lowest order in χ/γ and substitute these results into the reduced master equation (4.4) to obtain

$$\dot{\hat\rho}_{\rm rot} = \frac{-i}{\hbar}[\hat H_{\rm rot}, \hat\rho_{\rm rot}] - \frac{\chi^2}{2\gamma}[\hat n_b, [\hat n_b, \hat\rho_{\rm rot}]]. \tag{4.8}$$

In this equation we see an additional χ term arising. As we have $\gamma \gg \chi$, $\gamma t \gg 1$ and $\chi^2 t \gg \gamma$ this allows the good measurement limit. For the frequency converter we can write $\hat n_b$ in terms of $\hat J_z$ and obtain

$$\dot{\hat\rho}_{\rm FC} = -i\kappa[\hat J_x, \hat\rho_{\rm FC}] - \Gamma[\hat J_z, [\hat J_z, \hat\rho_{\rm FC}]], \tag{4.9}$$

where $\Gamma = \chi^2/2\gamma$ is the Zeno measurement parameter.

The last term in Eqs. (4.8) and (4.9) describes the effect of the measurement on the system in the limit of very good measurements. This double commutator term leads directly to the system becoming diagonalized in the basis which diagonalizes $\hat n_b$. Note that the rate of decay is the same as that given by the $\kappa = 0$ long-time solution given at the end of the preceding section.

V. REDUCED SYSTEM DYNAMICS

We now consider the effect of the measurement on either the Jaynes-Cummings two-level atom or the N_s level frequency converter system. We firstly note the equivalence of both systems when $N_s = 2$ or equivalently, when $N_p = 1$. In the selected basis for the Jaynes-Cummings two-level atom, Eq. (2.9), the free evolution term has matrix elements equivalent to J_x. The measurement operator n_b has the matrix elements $\frac{1}{2}I - J_z$. We readily see that for $N_s = 2$ the master equations for both systems are identical in their respective basis states. We first consider the frequency converter case and recover

the two-level-atom results when $N_s = 2$. As well we note that for the Jaynes-Cummings atom we can obtain the atomic level populations and coherences immediately from the basis states above.

The effect of measurement on the free dynamics of a two-level model equivalent to ours has already been discussed in Ref. [3]. The approach employed in that paper also gives insight to the $N_s \geq 2$ system. We consider the precession of an angular momentum vector defined to have components $x(t) = \langle J_x \rangle$, $y(t) = \langle J_y \rangle$, and $z(t) = \langle J_z \rangle$. The equation of motion of these components is readily obtained from the adiabatic master equation, see Ref. [3],

$$\frac{d}{dt}\begin{pmatrix} x \\ y \\ z \end{pmatrix} = \begin{pmatrix} -\Gamma & 0 & 0 \\ 0 & -\Gamma & -\kappa \\ 0 & \kappa & 0 \end{pmatrix}\begin{pmatrix} x \\ y \\ z \end{pmatrix}. \tag{5.1}$$

This equation applies for arbitrary $N_s \geq 2$ and the only N_s dependence comes from the initial vector $(0, 0, j)$ with $N_s = 2j + 1$. This dependence on N_s simply scales the magnitude of the vector, but does not change its behavior. However, only for $N_s = 2$ is there a simple relationship between $p_i(t)$, the initial-state occupation probability, and $z(t)$. We have

$$\begin{aligned} x(t) &= 0, \\ y(t) &= -\frac{\kappa j}{\Omega} e^{-\Gamma t/2}(e^{\Omega t/2} - e^{-\Omega t/2}), \\ z(t) &= \frac{j}{2\Omega} e^{-\Gamma t/2}[\,\Gamma(e^{\Omega t/2} - e^{-\Omega t/2}) \\ &\qquad + \Omega(e^{\Omega t/2} + e^{-\Omega t/2})], \end{aligned} \tag{5.2}$$

where $\Omega = \sqrt{\Gamma^2 - 4\kappa^2}$. For $\Gamma < 2\kappa$ the vector undergoes oscillations as it damps to the origin. For $\Gamma > 2\kappa$ all oscillations are damped and the angular momentum vector exponentially decays to the origin. For very large $\Gamma \gg \kappa$ we have

$$z(t) = je^{-\kappa^2 t/\Gamma} \tag{5.3}$$

and the vector undergoes a very slow exponential decay. We note for later reference that for a given rate of decay, we must scale $\Gamma \approx \kappa^2$, where κ is an effective strength of interaction. We also note that for any $\Gamma > 0^+$ and for all $N_s \geq 2$, the long-time value of the vector is $(0, 0, 0)$ which represents a system ensemble described by the identity matrix.

The evolution of an $N_s = 2$ system can be readily obtained by solving for the density-matrix elements in terms of the angular momentum vector components [3]. It is readily shown that the occupancy probability of the initial state $|I\rangle$ is given by

$$p_i(t) = \tfrac{1}{2} + z(t). \tag{5.4}$$

In Fig. 3 we show the effect of the measurement term on the evolution of the $N_s = 2$ level solution. We plot the initial-state occupancy probability for a range of measurement parameters Γ. Of interest is the transition from the free evolution oscillations for $\Gamma = 0$ to the exponentially damped behavior for large Γ. For very large Γ the system is trapped in the initial state. This is the Zeno effect in the strong, continuous measurement limit.

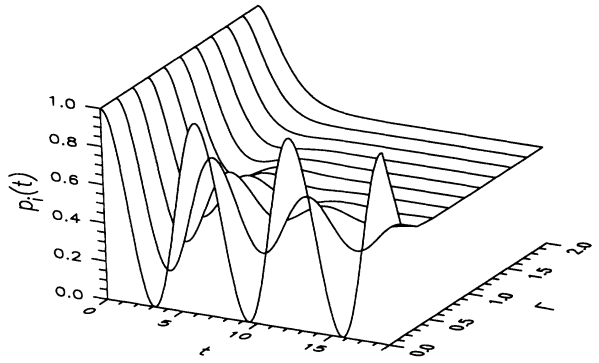

FIG. 3. The initial-state occupancy probability for the case $N_s = 2$ subject to increasingly strong measurement $\Gamma \geq 0$. This applies equally well to the two-level Jaynes-Cummings atomic system or the $N_p = 1$ photon frequency converter. For $\Gamma = 0$ we recover the free evolution. For long times we see the probability tending to the limiting value $1/N_s = \frac{1}{2}$. Note also the cessation of oscillations for $\Gamma = 2\kappa$ where $\kappa = 1$.

For the $N_s > 2$ case we have four constraint equations (three vector components and the constancy of the trace) applied to an $N_s \times N_s$ system of first-order partial differential equations. A numerical approach was adopted to examine the large N_s limit. However some insight into the expected behavior can be obtained as follows.

The matrix elements of $\rho(t)$ in the eigenbasis of J_z are defined by

$$\rho_{k,l} = \langle j, j - k + 1|\rho|j, j - l + 1\rangle. \tag{5.5}$$

The first two coupled equations are then

$$\begin{aligned} \dot{\rho}_{1,1} &= -i\kappa(J^x_{1,2}\rho_{2,1} - \rho_{1,2}J^x_{2,1}), \\ \dot{\rho}_{1,2} &= -i\kappa[J^x_{1,2}(\rho_{2,2} - \rho_{1,1}) - J^x_{3,2}\rho_{1,3}] - \Gamma\rho_{1,2}, \end{aligned} \tag{5.6}$$

where $J^x_{1,2} = \frac{1}{2}\sqrt{N_s - 1}$ and $J^x_{2,3} = \frac{1}{2}\sqrt{2(N_s - 2)}$. We proceed to obtain a "rate equation" description by adiabatically eliminating the off-diagonal elements, assuming Γ is sufficiently large. For $\Gamma \gg \kappa$ this gives

$$\dot{\rho}_{1,1}(t) = -\frac{\kappa^2 J^x_{1,2}}{\Gamma}[2J^x_{1,2}(\rho_{1,1} - \rho_{2,2}) + J^x_{3,2}(\rho_{1,3} + \rho_{3,1})]. \tag{5.7}$$

At $t = 0$, $\rho_{2,2}(0) = \rho_{1,3}(0) = \rho_{3,1}(0) = 0$ and thus

$$\dot{\rho}_{1,1}(t)|_{t=0} = -\frac{\kappa^2(N_s - 1)}{2\Gamma} = \dot{p}_i(t)|_{t=0}. \tag{5.8}$$

We see that the evolution away from the initial state occurs at the initial rate of $\kappa^2(N_s - 1)/2\Gamma$. The important factor is the linear dependence on N_s, which suggests

that we require the measurement parameter Γ to scale proportionally to N_s in order to obtain a Zeno effect for large N_s. This behavior is evident in the numerical results. For semiclassical systems with $N_s \to \infty$, the Zeno effect becomes unobservable.

In Fig. 4 we show the initial-state population $p_i(t)$ in the large N_s limit. We take $N_s = 10$ and vary Γ from 0 to 2. The free evolution of the system appears as the curve $\Gamma = 0$. Here we see a similar picture to the $N_s = 2$ case. Damped oscillations occur for small Γ but die out for large Γ. In all cases it is apparent that the long time limit of the population is tending to $1/N_s$, and for large Γ the initial state is trapped exhibiting the Zeno effect. The choice of $N_s = 10$ in Fig. 4 is illustrative of the system evolution for all large N_s. In particular, all oscillations have disappeared for $\Gamma > 2\kappa$. This was suggested by the results of Eq. (5.2). We see in Fig. 5 a plot of the initial-state occupancy probability for systems with $N_s = 2$, 10, and 15 and for the value $\Gamma = 2\kappa$. In this plot all oscillations have ceased, and the populations exhibit a smooth exponential decay to their respective long-time value of $1/N_s$.

The dominant feature in Fig. 5 is the enhanced rate of decay for increasing N_s. From the rate equation approach we expect that the initial rate of decay is proportional to N_s, and in fact equal to $\kappa^2(N_s - 1)/\Gamma$. We see this confirmed in Fig. 6 where we compare the rate of decay of the initial-state occupancy probability for three systems with $(N_s, \Gamma) = (2,2)$, $(10,20)$, and $(15,28)$ and with $\kappa = 1$. We do see similar initial rates of decay for these systems. This result then indicates that the size of the measurement parameter needed to produce a given Zeno effect, as shown in the rate of decay of the initial state population, must scale linearly with N_s.

In an experiment it will eventually be impossible to continue to scale $\Gamma \approx \kappa^2(N_s - 1)$ for increasing N_s. The size of Γ is limited by the resolution times and accuracy of the detector [4–6]. We therefore expect a divergence between this discrete model, which features arbitarily large Γ, and the experimental behavior of large N_s systems.

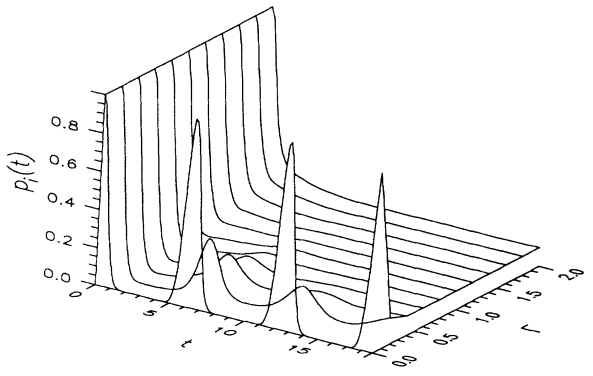

FIG. 4. The initial-state occupancy probability for the case $N_s \gg 2$ subject to increasingly strong measurement $\Gamma \geq 0$. This case only applies to the frequency converter. For $\Gamma = 0$ we recover the free evolution. For long times we see the probability tending to the limiting value $1/N_s$. Note also the cessation of oscillations for $\Gamma = 2\kappa$ where $\kappa = 1$.

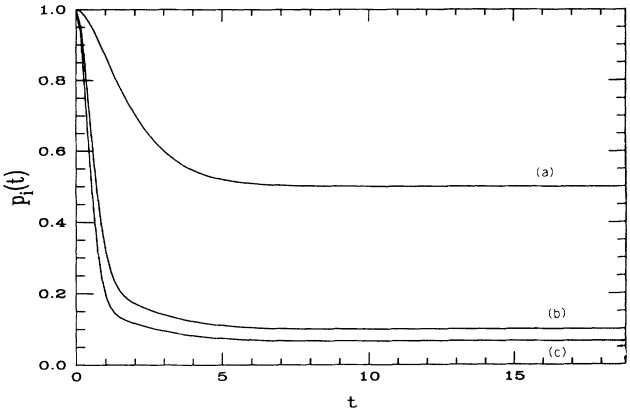

FIG. 5. We compare the rate of decay of the initial-state occupancy probability for three systems with (a) $N_s = 2$, (b) $N_s = 10$, and (c) $N_s = 15$ and for the value $\Gamma = 2\kappa$. In this plot all oscillations have ceased, and the populations exhibit a smooth exponential decay to their respective long-time value of $1/N_s$.

We investigate the range of applicability for this discrete model now.

The detector operates in the limit, $\gamma t \gg 1$ and $\chi^2 t \gg 2\gamma$. The resolution time for the detector is the time in which the b-mode photon coherences are destroyed and is given by

$$t_c \gg \frac{2\gamma}{\chi^2}. \tag{5.9}$$

This detector resolution time should be substantially shorter than typical evolution times in the system of interest. We gain some insight into the typical evolution time from the free evolution of the system. In this case (with $\Gamma = 0$) the initial-state occupancy probability is readily found to be [14]

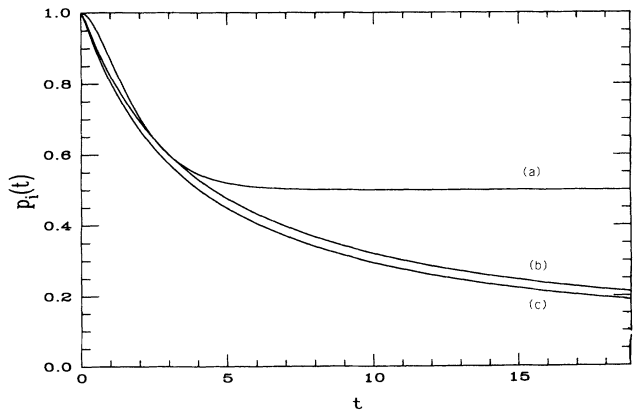

FIG. 6. We compare the rate of decay of the initial-state occupancy probability for three systems with (a) $(N_s, \Gamma) = (2,2)$, (b) $(N_s, \Gamma) = (10,20)$, and (c) $(N_s, \Gamma) = (15,28)$. We predict similar rates of decay for these systems given the result $\Gamma \approx \kappa^2(N_s - 1)$. With $\kappa = 1$ we do see roughly similar rates of decay for each pair (N_s, Γ). In each case the population tends to $1/N_s$.

$$p_i(t) = \left[\cos\left(\frac{\kappa t}{2}\right)\right]^{2(N_s-1)}, \tag{5.10}$$

as shown in Fig. 1 for the $N_s = 2, 40$ case. The initial-state occupancy becomes an increasingly narrow peak for large N_s with a half width of $\rho_{1,1}(\bar{t}) = \frac{1}{2}$ where

$$\bar{t} \approx \sqrt{\frac{2}{(N_s-1)\kappa^2}}. \tag{5.11}$$

We note that for large N_s we have $\bar{t} \to 0$. We require that the resolution time of the detector t_c needs to be substantially shorter than $\bar{t}$ to manifest the zeno effect. This requirement permits us to detect the system in some state before it has appreciably evolved away from that state. For this time to be much less than $\bar{t}$ we need

$$\kappa^2(N_s-1) \ll 2\Gamma^2. \tag{5.12}$$

This gives a heuristic limit to the size of the systems N_s that we would expect to be adequately modeled by this discrete model. The behavior shown in an experiment beyond this limit will show the cessation of the Zeno effect for increasing N_s. For increasing N_s systems will increasingly show free-evolution-type behavior over short times. This is in effect a semiclassical limit and thus we expect the Zeno effect to be unobservable in this limit.

VI. CONCLUSION

In this paper we show an experimental arrangement to demonstrate the quantum Zeno effect. We consider two possible systems of interest. The first is a Jaynes-Cummings two-level atom interacting with a cavity mode with annihilation operator b. The second is an N_s-level system made from two cavity modes, with annihilation operators a and b, interacting via a parametric interaction configured as a frequency converter. For these systems there is a direct correlation between the populations of the system of interest and the b-mode photon number. We employ this correlation to measure the initial-state system population.

We perform this measurement by establishing further correlations between the b mode and another cavity mode, with annihilation operator c. This interaction is via a quadratic coupling configured so as to be a quantum nondemolition measurement of the b-mode photon number. Subsequent photon counting measurements on the c mode are a continuous readout of the populations of the system of interest. We calculate the c-mode photon count signal-to-noise ratio and show that it is indeed a good measurement of the b-mode photon number, and hence of the system populations. We show that for strong measurements, the system populations are frozen. This is the quantum Zeno effect.

In the strong-measurement limit, the c mode is heavily damped by the photon counting and we are justified in adiabatically eliminating the c mode. We do this by treating the c mode as being only slightly perturbed from the vacuum. This elimination gives a reduced master equation describing the dynamics of the system of interest. We show a major feature of these reduced dynamics is a loss of coherence in the b-mode photon number basis. This basis is the pointer basis of the system, and this loss of coherence is the mechanism that enables the Zeno effect.

We present the dynamics of the system of interest for various measurement regimes and for various numbers of levels in the system. The dynamics feature a smooth transition in the initial-state population from the usual free evolution Rabi flopping to an exponential decay of probability for strong measurements. For systems with a large number of levels (N_s) the dynamics are similar but we must scale the measurement strength with N_s in order to get equivalent rates of decay. We use this scaling to demonstrate the regime for which this discrete level model will not adequately model real systems by considering the finite resolution time of our detection process.

APPENDIX: SIGNAL-TO-NOISE RATIO

In this appendix we consider the system-detector interaction with the free evolution turned off $\kappa = 0$. We make use of the results of Sec. III and perform selective measurements on the c-mode photon number and derive the relevant signal-to-noise ratio (SNR) of interest.

In the long-time limit $\gamma t \gg 1$ the c mode settles in a superposition of coherent states of the form $|-i\chi n/\gamma\rangle$. (There is also a short-time non-Markovian limit $\gamma t \ll 1$ which we do not consider here.) Once this equilibrium has been reached then photons are measured in the c mode as fast as they arrive. We expect therefore a linearly increasing photon count in the long-time limit. These results will be demonstrated below.

For the selective measurement we quote results from Ref. [18]. The probability of getting a readout of m photons at time t is

$$\begin{aligned} P(m,t) &= \sum_{n=0}^{\infty} \frac{x_n^m}{m!} e^{-x_n} P_b(n,0) \\ &= \left\langle \frac{\hat{x}_n^m}{m!} e^{-\hat{x}_n} \right\rangle_{b,0}, \end{aligned} \tag{A1}$$

where

$$x_n = \frac{\chi^2 n_b^2}{\gamma}\left(t - \frac{1}{\gamma}(e^{-\gamma t/2}-1)(e^{-\gamma t/2}-3)\right). \tag{A2}$$

In the limit $\gamma t \gg 1$ we have

$$\hat{x}_n = 2\Gamma t n_b^2, \tag{A3}$$

where we write $\Gamma = \chi^2/2\gamma$. In the long-time limit we can evaluate the average c-mode photon count in time t, $\bar{m}$, the variance in that count $V(m)$, and the signal-to-noise ratio of interest. We have

$$\begin{aligned} \bar{m} &= 2\Gamma t \langle \hat{n}_b^2 \rangle_{b,0}, \\ V(m) &= (2\Gamma t)^2 V_b(\hat{n}_b^2) + 2\Gamma t \langle \hat{n}_b^2 \rangle_{b,0}, \end{aligned} \tag{A4}$$

where $V_b(\hat{n}_b^2)$ is the variance of $\hat{n}_b^2$ evaluated in the initial

b-mode state. Here we see the expected time dependence of $\bar{m}$ in the long-time measurement limit. In the case where the b mode is initially in a photon number state, then $V_b(\hat{n}_b^2) = 0$.

We define the c-mode photon count signal-to-noise ratio (S) to be

$$S = \frac{\bar{m}^2}{V(m)}, \tag{A5}$$

and therefore, for sufficiently large Γt, $(2\Gamma t)^2 V_b(\hat{n}_b^2) \gg 2\Gamma t \langle \hat{n}_b^2 \rangle_{b,0}$ we have

$$S = \frac{\langle \hat{n}_b^2 \rangle_{b,0}^2}{V_b(\hat{n}_b^2)}. \tag{A6}$$

Here we see that the c-mode photon number readout is a good measurement of the b-mode photon number distribution. Thus, for a given time, a "good" measurement corresponds to large Γ.

For the case where the b mode is initially in a photon number state or when $(2\Gamma t)^2 V_b(\hat{n}_b^2) \ll 2\Gamma t \langle \hat{n}_b^2 \rangle_{b,0}$ we have

$$S_i = 2\Gamma t \langle \hat{n}_b^2 \rangle_{b,0}. \tag{A7}$$

[1] B. Misra and E. C. G. Sudarshan, J. Math. Phys. **18**, 757 (1977).
[2] A. Peres, Am. J. Phys. **48**, 931 (1980).
[3] G. J. Milburn, J. Opt. Soc. Am. **5**, 1317 (1988).
[4] K. Kraus, *States, Effects and Operations: Fundamental Notions of Quantum Theory* (Springer, Berlin, 1983).
[5] C. M. Caves and G. J. Milburn, Phys. Rev. A **36**, 5543 (1987).
[6] A. Barchielli, Nuovo Cimento B **74**, 113 (1983).
[7] W. M. Itano, D. J. Heinzen, J. J. Bollinger, and D. J. Wineland, Phys. Rev. A **41**, 2295 (1990).
[8] G. J. Milburn and M. J. Gagen (unpublished).
[9] A. Peres, Phys. Rev. D **39**, 2943 (1989).
[10] C. M. Caves, K. S. Thorne, K. W. P. Drever, N. D. Sandberg, and M. Zimmerman, Rev. Mod. Phys. **52**, 341 (1980).
[11] J. Tucker and D. F. Walls, Ann. Phys. (N.Y.) **52**, 1 (1969).
[12] G. J. Milburn, A. S. Lane, and D. F. Walls, Phys. Rev. A **27**, 2804 (1983).
[13] E. T. Jaynes and F. W. Cummings, Proc. IEE **51**, 89 (1963).
[14] B. Yurke, S. L. McCall, and J. R. Kaluder, Phys. Rev. A **33**, 4033 (1986).
[15] B. C. Sanders, Phys. Rev. A **40**, 2417 (1989).
[16] D. F. Walls, M. J. Collet, and G. J. Milburn, Phys. Rev. D **32**, 3208 (1985).
[17] G. J. Milburn and D. F. Walls, Phys. Rev. A **28**, 2646 (1983).
[18] G. J. Milburn and D. F. Walls, Phys. Rev. A **30**, 56 (1984).
[19] W. H. Louisell, *Quantum Statistical Properties of Radiation* (Wiley, New York, 1973).
[20] I. K. Mortimer and H. Risken (private communication).